their relative position. In particular they can be studied for $p=0$. The presence of p is to be superimposed without modifying their behavior.

This behavior confirms the previously obtained result on the system stability.

References

[1]Arrow, A. and Yost, D.J., "Large Angle of Attack Missile Control Concepts for Aerodynamically Controlled Missiles," *Journal of Spacecraft*, Vol. 14, Oct. 1977, pp.606-613.

[2]Christoffer, P.A.T., "Roll Attitude Control of a Missile Having a Strong Aerodynamic Nonlinearity," *International Journal of Control*, Vol. 31, Feb. 1980, pp. 209-218.

[3]Etkin, B., *Dynamics of Flight*, John-Wiley, New York, 1962, Chap. 4.

[4]Howe, R.M., "Coordinate Systems for Solving the Three Dimensional Flight Equations," WADC TN-55747, June 1956.

[5]Wardlaw, A.B. Jr. and Morrison, A.M., "Induced Side Forces at High Angles of Attack," *Journal of Spacecraft*, Vol. 13, Oct. 1976, p. 5890-593.

Miss Distance of Proportional Navigation Missile with Varying Velocity

W. R. Chadwick*
Naval Surface Weapons Center, Dahlgren, Virginia

Introduction

In most of the published work on proportional navigation guidance, the assumption is made that the missile and target velocities remain constant.[1,2] This ensures a collision against the nonmaneuvering target if the missile maintains a constant relative bearing while closing in range. To achieve this constant bearing angle, the proportional navigation missile thus attempts to null the line-of-sight rate.[3]

Axial acceleration or slowdown may seriously influence the performance of the proportional navigation missile.[4] There are two main reasons for this. First, the lateral acceleration and miss distance performance of the missile depend strongly on the effective navigation constant $\tilde{N}$, which varies with speed. Velocity compensation is thus usually necessary to ensure that $\tilde{N}$ remains within the desired range of 3 to 5.[5] The second direct kinematic effect of nonconstant axial velocity is that it prevents the missile from achieving a constant bearing or rectilinear collision course to the target. An important example here is the short-range engagement with large crossing angle that occurs during a period of large boost acceleration. In this case, however, the magnitude and duration of the boost acceleration are usually known and a simple lateral acceleration correction may be computed and added to the primary guidance signal to compensate for axial acceleration.[6] A more difficult situation may arise at longer ranges and higher altitudes when the missile sustainer motor burns out just before intercept. The missile will normally have limited maneuver capability and a slow dynamic response rate at these high altitudes and, thus, may be unable to entirely compensate for the resulting sudden axial slowdown. A suitable velocity compensation scheme is more difficult in this case. This is because the "time to go" at thrust cutoff and the resulting missile slowdown rate are not precisely known. The missile's heading at cutoff is also unknown. In addition, of course, the absence of any theoretical results on the influence of axial slowdown on miss distance performance further complicates the task of devising a compensation scheme for the above case. The present work provides these results.

The analysis is confined to the noise-free case of a nonmaneuvering crossing air target and considers a single-lag missile having an effective navigation constant of four and unlimited lateral acceleration capability. An approximate analytical solution is developed for the miss distance which consists of two parts. The first is associated directly with the kinematic effects of missile slowdown following sustain thrust cutoff, while the second is due to missile heading error at thrust cutoff. This second component of the miss is already known for the constant-speed case as a linear function of heading error for any integer navigation constant.[1] The task here was to estimate typical thrust cutoff heading errors caused by varying velocity during the sustain thrust phase. This problem is solved using a simplification of the general analysis which neglects higher-order dynamics.

It is shown that if sudden missile slowdown caused by sustain thrust cutoff occurs within three missile time constants of intercept against the high-speed crossing target, the unbiased proportional navigation missile will usually miss behind the target centroid.

As a final note, it is repeated that the present analytical solution for the miss distance due to heading error has been available for a number of years. On the other hand, to the author's knowledge, no previously published solution is available for the miss due to missile acceleration or slowdown.

The Differential Equation

The engagement geometry for the longitudinally accelerating proportional missile against a constant velocity crossing target is shown in Fig. 1. The x axis is inclined to the initial line of sight at ϕ_0, where

$$V_0\sin\phi_0 = V_T\sin\psi_T \tag{1}$$

Thus, at thrust cutoff, ϕ_0 defines the constant bearing course, or the rectilinear collision course which would be necessary for the missile to intercept the target without further maneuver if the velocity following thrust cutoff were to remain constant at V_0. Following cutoff, however, the linear velocity law

$$V = V_0 + at \tag{2}$$

is assumed, with the missile's initial heading having the small perturbation ϵ relative to ϕ_0. In the following analysis, the quantity ϵ is taken to be zero only when V is assumed to be constant prior to thrust cutoff. The heading error ϵ is estimated later in the section entitled "Missile Heading at the End of the Thrust Phase."

The rate of change of the missile flight-path angle, assuming a single-lag time constant τ, is given by[7]

$$\frac{d\gamma}{dt} = N\left[\frac{d\sigma}{dt}\Big/ 1+s\tau\right] \tag{3}$$

where $s=d/dt$. Assuming small deviations in γ and σ, Eq. (3) may be written

$$\tau\frac{d^3y}{dt^3}+\frac{d^2y}{dt^2} = NV\frac{d}{dt}\left[\frac{y'_T-y'}{x'_T-x'}\right] \tag{4}$$

where, from Fig. 1 and Eq. (2)

$$x' = \left(V_0t+\frac{at^2}{2}\right)\cos\phi_0 - y\sin\phi_0 \tag{5}$$

Received Jan. 6, 1984; revision received Oct. 22, 1984.

*Research Associate, Weapons Systems Department.

$$y' = \left(V_0 t + \frac{at^2}{2}\right)\sin\phi_0 + y\cos\phi_0 \tag{6}$$

$$x_T = R_0 - V_T\cos\psi_T t \tag{7}$$

$$y_T = V_T\sin\psi_T t \tag{8}$$

Performing the differentiation indicated by Eq. (4) and using Eq. (1)

$$\tau\frac{d^3y}{dt^3} + \frac{d^2y}{dt^2} = \bar{N}\left[\left(\frac{dy}{dt} + at\tan\phi_0\right)\left(\frac{\Delta\dot{x}'}{\Delta x'}\right) - \left(y + \frac{at^2}{2}\tan\phi_0\right)\left(\frac{\Delta\dot{x}'}{\Delta x'}\right)^2\right] \tag{9}$$

where we have employed the classical definition of the effective navigation constant[5]

$$\bar{N} = -\frac{NV\cos\phi_0}{\Delta\dot{x}'} \tag{10}$$

with

$$\Delta\dot{x}' = \dot{x}_T' - \dot{x}' \tag{11}$$

For the single-lag proportional navigation missile with unlimited lateral acceleration capability, Eq. (9) is exact within the framework of small-angle point mass kinematics. However, to obtain a useful analytical solution of this equation, some simplification of the $\Delta x'$ coefficients is required. The most obvious is to replace the horizontal closing rate $\Delta\dot{x}'$ by a constant based on the missile's average velocity. That is

$$\Delta\dot{x}' = -\bar{V} \tag{12}$$

$$\Delta x' = \bar{V}(T-t) \tag{13}$$

$$\bar{V} = \left(V_0 + \frac{aT}{2}\right) + V_T\cos\psi_T \tag{14}$$

with T denoting the total time of flight or time to go from thrust cutoff.

With these approximations and a change of independent variable from t to ρ, where

$$\rho = (T-t)/\tau \tag{15}$$

is the nondimensional time to go, Eq. (9) becomes

$$-\rho^2\frac{d^3y}{d\rho^3} + \rho^2\frac{d^2y}{d\rho^2} - 4\rho\frac{dy}{d\rho} + 4y = R(\rho) \tag{16}$$

where

$$R(\rho) = 2\tau^2 at\tan\phi_0(\rho^2 - \rho_0^2) \tag{17}$$

and the initial conditions, from Fig. 1 and Eq. (15), are

$$y = 0, \quad \frac{dy}{d\rho} = -V_0\tau\epsilon, \quad \frac{d^2y}{d\rho^2} = 0, \quad \rho = \rho_0 \text{ or } t = 0 \tag{18}$$

for the specific case $\bar{N} = 4$.

Solution of the Differential Equation

Noting that $y = \rho$ is one solution of Eq. (16) in the case $R(\rho) = 0$, denote the complete general solution by[7]

$$y = S\rho \tag{19}$$

where $S = S(\rho)$. Differentiating

$$\frac{dy}{d\rho} = S + \rho\frac{dS}{d\rho} \tag{20}$$

$$\frac{d^2y}{d\rho^2} = 2\frac{dS}{d\rho} + \rho\frac{d^2S}{d\rho^2} \tag{21}$$

$$\frac{d^3y}{d\rho^3} = 3\frac{d^2S}{d\rho^2} + \rho\frac{d^3S}{d\rho^3} \tag{22}$$

and substituting into Eq. (16) results in the following second-order equation for $dS/d\rho$

$$\rho\frac{d^2}{d\rho^2}\frac{dS}{d\rho} + (3-\rho)\frac{d}{d\rho}\frac{dS}{d\rho} + 2\frac{dS}{d\rho} = -\frac{R}{\rho^2} \tag{23}$$

One of the two independent homogeneous solutions of Eq. (23) is

$$\frac{dS}{d\rho} = 1 - \frac{2}{3}\rho + \frac{\rho^2}{12} = F(\rho) \tag{24}$$

which may be verified by direct substitution. Thus, as before, let the complete solution of the equation be

$$\frac{dS}{d\rho} = P(\rho)F(\rho) \tag{25}$$

Now differentiate with respect to ρ

$$\frac{d}{d\rho}\frac{dS}{d\rho} = PF' + FP' \tag{26}$$

$$\frac{d^2}{d\rho^2}\frac{dS}{d\rho} = PF'' + 2P'F' + FP'' \tag{27}$$

where the prime denotes differentiation with respect to ρ and where we have written P for $P(\rho)$, etc. Now substitute into Eq. (23)

$$\frac{d}{d\rho}\left(\frac{dP}{d\rho}F^2\rho^3e^{-\rho}\right) = -RFe^{-\rho} \tag{28}$$

and integrate twice

$$\frac{dP}{d\rho}F^2\rho^3e^{-\rho} = -\int_{\rho_0}^{\rho} RFe^{-\rho}d\rho + P'(\rho_0)F^2(\rho_0)\rho_0^3e^{-\rho_0} \tag{29}$$

$$P = -\int_{\rho_0}^{\rho}\frac{e^y}{F^2y^3}\int_{\rho_0}^{y} RFe^{-x}dxdy + P'(\rho_0)F^2(\rho_0)\rho_0^3e^{-\rho_0}\int_{\rho_0}^{\rho}\frac{e^x}{F^2x^3}dx + P(\rho_0) \tag{30}$$

where the initial values of P and P' may be obtained from Eq. (18)

$$P(\rho_0) = -\frac{V_0\tau\epsilon}{F(\rho_0)\rho_0} \tag{31}$$

$$P'(\rho_0) = \frac{V_0\tau\epsilon}{F(\rho_0)}\left[\frac{2}{\rho_0^2} + \frac{F'(\rho_0)}{F(\rho_0)}\right] \tag{32}$$

Miss Distance

The miss distance

$$M = (y_T' - y)_{\rho=0} \tag{33}$$

as shown in Fig. 1, may be written

$$M = (aT^2/2)\sin\phi_0 - y(0)\cos\phi_0 \tag{34}$$

from Eqs. (6) and (8) and from the definition of the initial constant bearing course.

Now, from Eq. (20), it is possible to write

$$\rho\left(S+\rho\frac{\mathrm{d}S}{\mathrm{d}\rho}\right)_{\rho=0}=0 \tag{35}$$

assuming $\mathrm{d}y/\mathrm{d}\rho$ remains finite at $\rho=0$. But $\rho S(\rho)=y$, from Eq. (19), and, therefore,

$$y(0)=-\rho^2\left(\frac{\mathrm{d}S}{\mathrm{d}\rho}\right)_{\lim\rho\to 0} \tag{36}$$

$$\therefore y(0)=-(\rho^2 FP)_{\lim\rho\to 0} \tag{37}$$

$$y(0)=\rho^2 F\int_{\rho_0}^{\rho}\frac{e^y}{F^2y^3}\int_{\rho_0}^{y}RFe^{-x}\mathrm{d}x\mathrm{d}y$$

$$-P'(\rho_0)F^2(\rho_0)\rho_0^3e^{-\rho_0}\rho^2F\int_{\rho_0}^{\rho}\frac{e^x}{F^2x^3}\mathrm{d}x$$

$$-\rho^2FP(\rho_0);\quad \lim\rho\to 0 \tag{38}$$

For the simple $R(x)$ and $F(x)$ polynomials of Eqs. (17) and (24), respectively, it is easy to show that, in the limit, as ρ approaches zero, Eq. (38) may be written

$$y(0)=\frac{1}{2}\int_0^{\rho_0}R(x)F(x)e^{-x}\mathrm{d}x+\frac{P'}{2}(\rho_0)F^2(\rho_0)\rho_0^3e^{-\rho_0} \tag{39}$$

Performing the integration, with $P'(\rho_0)$ from Eq. (32),

$$y(0)=\frac{\tau^2}{2}a\tan\phi_0\rho_0^2e^{-\rho_0}\left(1-\frac{\rho_0}{3}\right)-\frac{aT^2}{2}\tan\phi_0$$

$$+V_0\tau\epsilon\rho_0e^{-\rho_0}\left(1-\rho_0+\frac{\rho_0^2}{6}\right) \tag{40}$$

Thus, from Eq. (34), the miss is

$$M=-\frac{\tau^2a}{2}\frac{V_T}{V_0}\sin\psi_T\rho_0^2e^{-\rho_0}\left(1-\frac{\rho_0}{3}\right)$$

$$-V_0\tau\epsilon\cos\phi_0\rho_0e^{-\rho_0}\left(1-\rho_0+\frac{\rho_0^2}{6}\right) \tag{41}$$

Before discussing this result we estimate below the general level of ϵ to be expected at the end of the sustainer thrust phase, assuming simple unbiased proportional navigation guidance.

Missile Heading at the End of the Thrust Phase

The quantity ϵ at the termination of the sustain thrust phase has been defined as

$$\epsilon=\gamma-\phi \tag{42}$$

where γ is the flight heading and ϕ denotes the initial constant bearing angle. An estimate of ϵ may be obtained by assuming that the time of flight is much larger than the missile time constant. If we thus neglect τ in the previous analysis, the trajectory, and, therefore, ϵ, of the unbiased proportional navigation missile with varying velocity, may easily be determined. Accordingly, with time now assumed to start at the commencement of the sustain thrust phase and T denoting the total time to intercept, Eqs. (16) and (17) become

$$(T-t)\frac{\mathrm{d}^2y}{\mathrm{d}t^2}+4(T-t)\frac{\mathrm{d}y}{\mathrm{d}t}+4y=2a\tan\phi_0(t^2-2Tt) \tag{43}$$

where, in order to determine the approximate kinematic state of the missile at thrust cutoff, just before intercept, we may assume zero initial conditions. As in the previous work, let V_0 and ϕ_0 denote conditions at $t=0$ and let a denote the longitudinal acceleration of the missile under sustain thrust. Then

$$V=V_0+at \tag{44}$$

and

$$\sin\phi_0=\frac{V_T}{V_0}\sin\psi_T \tag{45}$$

The complete solution of Eq. (43) is relatively simple

$$y=-\frac{2}{3}a\tan\phi_0T^2\mu^3\left(1-\frac{\mu}{4}\right) \tag{46}$$

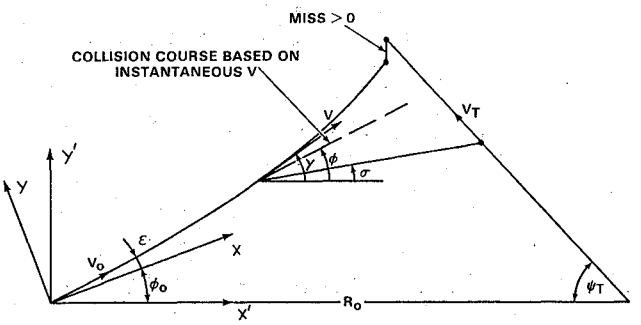

Fig. 1 Engagement geometry.

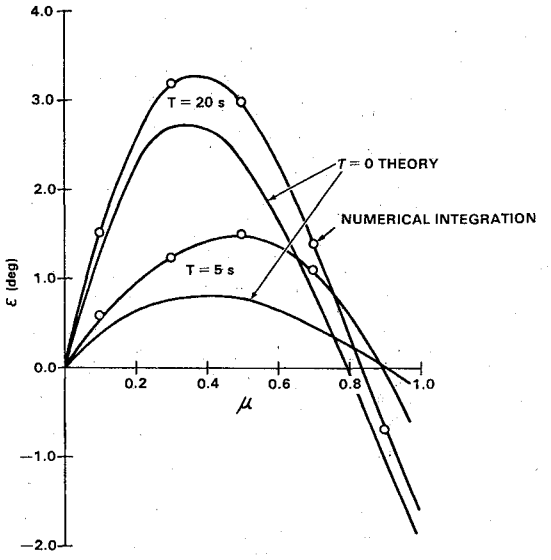

Fig. 2 Heading error due to longitudinal acceleration.

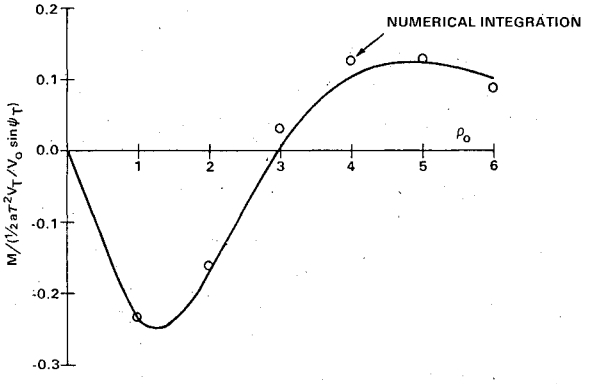

Fig. 3 Normalized miss due to longitudinal deceleration.

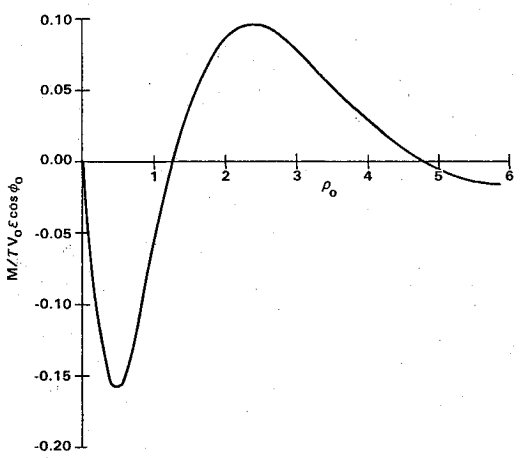

Fig. 4 Normalized miss due to heading error.

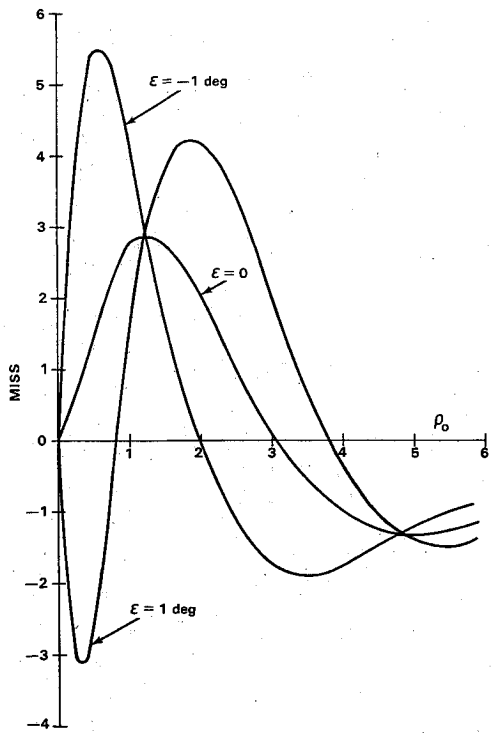

Fig. 5 Miss due to longitudinal deceleration and heading error.

where

$$\mu = t/T \tag{47}$$

as may be checked by direct substitution. The flight heading

$$\gamma = \phi_0 + (\dot{y}/V) \tag{48}$$

may be evaluated by differentiating Eq. (46)

$$\gamma = \phi_0 - \frac{2a}{V}\tan\phi_0 T\mu^2\left(1 - \frac{\mu}{3}\right) \tag{49}$$

Now, using Fig. 1, the constant bearing angle or instantaneous collision heading corresponding to the velocity V at time t is given by

$$V\sin(\phi - \sigma) = V_T\sin(\psi_T + \sigma) \tag{50}$$

which may be written

$$\sin\phi = \frac{V_T}{V}\sin\psi_T + \frac{\sigma}{V}(V_T\cos\psi_T + V\cos\phi) \tag{51}$$

The small angle σ is given by

$$\bar{V}(T-t)\sigma = V_T\sin\psi_T t - (x\sin\phi_0 + y\cos\phi_0) \tag{52}$$

which, upon substituting $x = V_0 t + \frac{1}{2}at^2$, and using Eq. (45), may be written

$$\bar{V}(T-t)\sigma = -\tfrac{1}{2}at^2\sin\phi_0 - y\cos\phi_0 \tag{53}$$

If we now assume that the horizontal closing velocity in Eq. (53) cancels the grouping of velocity terms in Eq. (51), and use Eq. (46) for y, the required collision heading is

$$\phi = \sin^{-1}\left\{\frac{V_0\sin}{V}\phi_0\left[1 - \frac{aT\mu^2}{V_0}\frac{(1 - 4\mu/3 + \mu^2/3)}{2(1-\mu)}\right]\right\} \tag{54}$$

Figure 2 compares the ϵ of this zero lag theory, obtained by subtracting Eq. (54) from Eq. (49), with results obtained by integrating Eq. (9) numerically for the case $V_0 = V_T = 2000$ ft/s, $\psi_T = 45$ deg, $\tau = 1$ s, and $a = 32$ ft/s^2. The simple theory, which is quite satisfactory for large values of T, shows that if thrust cutoff occurs shortly before intercept, as μ approaches 1, then ϵ in the range ± 1 deg should be expected.

Discussion

The two components of Eq. (41) are the miss due to the missile's longitudinal deceleration following thrust cutoff ($a < 0$) and the miss due to the missile's heading error at thrust cutoff. Figure 3 compares the first of these components with results obtained by integrating Eq. (9) numerically for the case $V_0 = V_T = 2000$ ft/s, $\psi_T = 45$ deg, $\tau = 1$ s, and $a = -150$ ft/s^2. Clearly the basic assumptions of the theory are entirely satisfactory. Note that Fig. 3 shows normalized miss against ρ_0, where ρ_0 denotes time to go at thrust cutoff divided by missile time constant. Accordingly, Fig. 3 may be used to predict the miss due to any combination of missile speed, cutoff time, axial deceleration or speedup, and time constant; and for any target speed and crossing angle. An important feature of Fig. 3 is that the decelerating proportional navigation missile ($a < 0$), with unlimited lateral maneuver capability and zero heading error at thrust cutoff, will experience a positive miss distance whenever the slowdown phase commences within three missile time constants or intercept. During such encounters a large positive incidence may be expected to develop (see Fig. 1), which will increase the final orientation of the missile's longitudinal axis relative to the target flight path. For $\rho_0 > 3$ the situation is reversed.

The second component of Eq. (41), the normalized miss due to heading error at thrust cutoff, is shown in Fig. 4. This component exhibits zeros at $\rho_0 = 3 \pm \sqrt{3}$ and becomes very small for $\rho_0 > 5$.

The total miss (in feet) is shown in Fig. 5 for the case $V_0 = V_T = 2000$ ft/s, $\psi_T = 45$ deg, and $a = -32$ ft/s^2. Thus, if thrust cutoff occurs shortly before intercept ($\rho_0 < 4$), the axially decelerating proportional navigation missile will experience a large positive miss distance irrespective of the sense of the cutoff heading error.

Conclusions

It has been shown that if sudden missile deceleration caused by sustain thrust cutoff occurs within three missile time constants of intercept, against the high-speed crossing air target, then the unbiased proportional navigation missile will miss behind the target centroid. Furthermore, typical missile heading errors at the end of the sustainer thrust phase will

usually increase this positive miss distance. The unbiased proportional navigation missile experiencing sustain thrust cutoff shortly before intercept may thus develop a large positive angle of attack during terminal encounter. For large crossing angles this may rotate the missile longitudinal axis to the extent that the effectiveness of the warhead is significantly reduced.

References

[1]Cornford, B.A. and Bain, M.A., "The Kinematics of Proportional Navigation Courses for a Missile with a Time Lag," Royal Aircraft Establishment, England, Tech. Note GW85, Oct. 1950.

[2]Paarman, L.O., Farone, J.M., and Smoots, G.W., "Guidance Law Handback for Classical Proportional Navigation," IIT Research Institute, Chicago, Ill, Rept. GACIAC HB-78-01, June 1978.

[3]Pastrick, H.L., Seltzer, S.M., and Warren, M.E., "Guidance Laws for Short-Range Tactical Missiles," *Journal of Guidance and Control,* March-April 1981, pp. 98-108.

[4]Arbenz, K., "Proportional Navigation of Nonstationary Targets," *IEEE Transactions on Aerospace and Electronic Systems,* July 1970, pp. 455-457.

[5]Nesline, F.W. and Zarchan, P., "A New Look at Classical vs Modern Homing Missile Guidance," *Journal of Guidance and Control,* Jan.-Feb. 1981, pp. 78-85.

[6]Smith, W.M., "Preliminary Trajectory Shaping Policy for SM2 Block 11 ER/HAW," General Dynamics, Pomona, Calif., TM 6-331-119.30.1, Jan. 1979.

[7]Chadwick, W.R., "A Theoretical Analysis of Collision Course Navigation with Command Guidance," Weapons Research Establishment, South Australia, Tech. Note SAD 141, Dec. 1964.

Guidance Performance Analysis with In-Flight Radome Error Calibration

William R. Yueh*
Northrop Electronics Division
Hawthorne, California
and
Ching-Fang Lin†
Boeing Company, Seattle, Washington

Introduction

MISSILE homing performance can be seriously degraded by boresight radome errors whose slopes generally show large variations. Thus, to increase homing performance and target intercept capability, in-flight radome error calibration is essential to overcome the restrictions imposed by radome errors.[1-5] This Note presents a self-learning network scheme with an adaptive real-time estimation using a Kalman filter bank design for the switching environment for high-altitude, high-speed threat.

Adaptive Radome Estimator Design

An adaptive Kalman filtering bank in the switching environment is used to realize the changing processes in a radome slope. The rate of switching is assumed to be considerably slower than that of the boresight error (observation) sampling rate. That is, by assuming the rate of positive-negative radome slope switching to be smaller than the data sampling rate, the estimation scheme can be reduced to the design of a bank of Kalman filters, each matched to a certain radome slope configuration. Actually, following the adaptive filter formulation in Refs. 6-8, the random switching of the unreliable plant, i.e., the radome slope is modeled by a semi-Markov process.

A semi-Markov process is a probabilistic system that makes its state transitions according to the transition probability matrix of a conventional Markov process. However, the amount of time spent in each state before the next transition to a different state is a random variable. It is this property of a random switching time that distinguishes the more general semi-Markov process from a Markov process. The multiple states mentioned above are actually chosen to typify the radome slope in the positive, zero, or negative slope regions. Thus, by proper choice of the state and modeling of the transition processes, we hope to realize the variations of the radome slope as a randomly switching, semi-Markov process.

The general adaptive filter, as shown in Fig. 1, essentially consists of a bank of three Kalman filters, each matched to a possible plant configuration U_i $(i=1,2,3)$. The filter outputs are weighted by a time-varying a posteriori probability to obtain the radome error slope estimate. The bank of three Kalman filters has the deterministic inputs $U_1=U_+=0.02$ deg/deg, $U_2=U_0=0.0$ deg/deg, and $U_3=U_-=-0.02$ deg/deg to characterize the three plant configurations in the positive, zero, and negative slope regions, respectively. That is, the filter estimates from each filter in the bank are further weighted by calculating the a posteriori hypothesis probabilities. It is the probability of a given hypothesis that the radome slope is around certain U_i value, being true conditioned upon the past measurements. Since during actual flight the unknown plant configuration (due to polarization effect) might randomly switch at random times, we have to model the random switching of the radome slope parameters as a semi-Markov process. The a posteriori hypothesis testing involves the three conditional probabilities

$$P_{1,k+1}=P_+(U_{k+1}=U_+\,|Z_{k+1})$$
$$P_{2,k+1}=P_0(U_{k+1}=U_0\,|Z_{k+1})$$
$$P_{3,k+1}=P_-(U_{k+1}=U_-\,|Z_{k+1}) \qquad (1)$$

where Z_{k+1} denotes the collective events of all the past measurement history up to time t_{k+1}, i.e.,

$$Z_{k+1}=\{z_1,z_2,\ldots z_k,z_{k+1}\}=\{Z_k,z_{k+1}\} \qquad (2)$$

Equation (1) actually states that for a new boresight datum z_{k+1} that just comes in, we want to test a global hypothesis to see whether the datum indicates that the plant configuration, or the radome slope, is near the positive, zero, or negative slope region. It is a global instead of local hypothesis because it depends on the time history of the data, as shown in Eq. (2). Thus, the a posteriori conditional probabilities should be calculated recursively to reflect all the past data dependence. The detailed formulations are given in Refs. 6 and 7 and are shown below for $i=1,2,3$, as

$$P_{i,k+1}=P(z_{k+1}\,|U_{k+1}=U_i,Z_k)\times \text{normalizing factor}$$
$$\times\sum_{j=1}^{3}[P_{j,k}\times\mathcal{K}_{ij}(t_{k+1}-t_k)] \qquad (3)$$

in terms of the recursive time index k. The normalizing factor is the inverse of the sum of the three a posteriori conditional probabilities. The transition matrix $\mathcal{K}_{ij}$ from state U_i to U_j is symmetric and is based on the semi-Markov statistics. This

Received Oct. 12, 1984; revision received Feb. 19, 1985.

*Senior Research Engineer. Member AIAA.
†Lead Engineer, Flight Controls Technology. Member AIAA.